

# Mixing in the Solar Nebula: Implications for Isotopic Heterogeneity and Large-Scale Transport of Refractory Grains

Alan P. Boss

DTM, Carnegie Institution, 5241 Broad Branch Road, N.W., Washington, D.C.  
20015-1305, U.S.A.

---

## Abstract

The discovery of refractory grains amongst the particles collected from Comet 81P/Wild 2 by the Stardust spacecraft (Brownlee et al. 2006) provides the ground truth for large-scale transport of materials formed in high temperature regions close to the protosun outward to the comet-forming regions of the solar nebula. While accretion disk models driven by a generic turbulent viscosity have been invoked as a means to explain such large-scale transport, the detailed physics behind such an  $\alpha$  viscosity remains unclear. We present here an alternative physical mechanism for large-scale transport in the solar nebula: gravitational torques associated with the transient spiral arms in a marginally gravitationally unstable disk, of the type that appears to be necessary to form gas giant planets. Three dimensional models are presented of the time evolution of self-gravitating disks, including radiative transfer and detailed equations of state, showing that small dust grains will be transported upstream and downstream (with respect to the mean inward flow of gas and dust being accreted by the central protostar) inside the disk on time scales of less than 1000 yr inside 10 AU. These models furthermore show that any initial spatial heterogeneities present (e.g., in short-lived isotopes such as  $^{26}\text{Al}$ ) will be homogenized by disk mixing down to a level of  $\sim 10\%$ , preserving the use of short-lived isotopes as accurate nebular chronometers, while simultaneously allowing for the spread of stable oxygen isotope ratios. This finite level of nebular spatial heterogeneity appears to be related to the coarse mixing achieved by spiral arms, with radial widths of order 1 AU, over time scales of  $\sim 1000$  yrs.

## Key words:

solar nebula, short-lived radioactivities, oxygen isotopes, refractory inclusions, comets, chronometry, accretion disks

---

Email address: boss@dtm.ciw.edu (Alan P. Boss).

URL: <http://www.dtm.ciw.edu/boss> (Alan P. Boss).

## 1 Introduction

Comets have long been recognized as relatively pristine repositories of particles from the early solar system, and combined with primitive chondritic meteorites, these objects represent the best records we have of the events in the solar nebula some 4.57 Gyr ago. For this very reason, the Stardust Mission to Comet 81P/Wild 2 was conceived and launched to sample the particles in the coma of this Jupiter family comet (JFC). JFCs are believed to have formed in the Kuiper Belt, just beyond Neptune's orbit, and so Wild 2 is thought to be a sample of the outermost planet-forming region of the solar nebula. The discovery of refractory grains by Stardust (Brownlee et al. 2006) therefore provided proof that grains that formed in high temperature regions of the disk, presumably close to the protosun, were able to be transported outward tens of AU to the JFC-forming region prior to their incorporation in comets (see also Nuth & Johnson 2006).

There are two possibilities for the outward transport of the high temperature minerals found by Stardust. First, refractory grains formed close to the protosun may have been carried upward by the protosun's bipolar outflow and lofted onto trajectories that would return them to the surface of the solar nebula at much greater distances (Shu et al. 2001). Bipolar outflows are known to occur, but the lofting of grains and their return to the outer disk are processes that are not constrained by astronomical observations, though the Stardust discoveries can be interpreted as proof of this possibility. Alternatively, refractory solids might have been transported outward to comet-forming distances by mixing processes within the solar nebula, such as generic accretion disk turbulence (Gail 2002; Ciesla & Cuzzi 2006; Tschamuter & Gail 2007; Ciesla 2007), or the actions of spiral arms in a marginally gravitationally unstable nebula (Boss 2004, 2007). The magnetorotational instability (MRI) in an ionized disk is often considered to be the physical mechanism responsible for disk evolution and the source of the disk's effective  $\alpha$  viscosity. However, MRI effects are limited to the disk's surfaces and its innermost and outermost regions by the need for appreciable fractional ionization. The ionized surface layers are thought to be dominated by the inward flow of gas accreting onto the protostar. The disk's midplane is essentially neutral in the planet-forming region from  $\sim 1$  to  $\sim 15$  AU, preventing the MRI from serving as a driver of midplane disk evolution in this key region (e.g., Matsumura & Pudritz 2006). Gravitational torques in a marginally gravitationally unstable disk, however, are able to drive global angular momentum transport throughout the dead zone, and in fact periods of gravitational instability may well be regulated by the pile-up of disk gas on the edge of the dead zone by the action of the MRI in the more ionized regions of the disk.

Astronomical observations of disks around young stars often find evidence for

crystalline silicate grains at distances ranging from inside 3 AU to beyond 5 AU, in both the disk's midplane and its surface layers (Meru et al. 2007). These grains could have been produced through thermal annealing of amorphous grains by hot disk temperatures reached only within the innermost disk, well inside 1 AU. Crystalline and amorphous silicate grains thus appear to require large-scale transport as well. In addition, isotopic evidence suggests (e.g., Bizzarro, Baker & Haack 2004) that some Allende chondrules formed with an  $^{26}\text{Al}/^{27}\text{Al}$  ratio similar to that of calcium, aluminum-rich inclusions (CAIs). Chondrule formation thus appears to have begun shortly after CAI formation, and to have lasted for 1 Myr to 4 Myr (Amelin et al. 2002). While chondrules are generally believed to have been melted by shock-front heating at asteroidal distances (e.g., Desch & Connolly 2002), CAIs are thought to have formed much closer to the protosun, again because of their refractory compositions. Transport of solids from the inner solar nebula out to asteroidal distances thus seems to be required in order to assemble chondrules, CAIs, and matrix grains into the chondritic meteorites (Boss & Durisen 2005).

While the evidence for large-scale transport is clear, the degree of mixing of the nebula gas and solid has been less clear for some time. Isotopic evidence has been presented for both homogeneity (e.g., Hsu, Huss & Wasserburg 2003) and heterogeneity (e.g., Simon et al. 1998) of short-lived radioisotopes (SLRI) such as  $^{26}\text{Al}$  and  $^{60}\text{Fe}$  in the solar nebula. The solar system's  $^{60}\text{Fe}$  must have been synthesized in a supernova (Mestefauji, Lugmair & Hoppe 2005; Tachibana et al. 2006) and then injected either into the presolar cloud (Vanhala & Boss 2002) or onto the surface of the solar nebula (e.g., Boss 2007), processes that both lead to initially strongly heterogeneous distributions. The initial degree of homogeneity of the SLRI is crucial if  $^{26}\text{Al}/^{27}\text{Al}$  ratios are to be used as precise chronometers for the early solar system (Bizzarro et al. 2004; Halliday 2004; Krot et al. 2005; Thrane et al. 2006).

The degree of uniformity is equally murky even for stable isotopes. For samarium and neodymium isotopes, both nebular homogeneity and heterogeneity have been claimed, depending on the objects under consideration (Andreasen & Sharma 2007), e.g., ordinary versus carbonaceous chondrites. However, osmium isotopes seem to require a high degree of homogeneity in both ordinary and carbonaceous chondrites (Yokoyama et al. 2007). The three stable isotopes of oxygen, on the other hand, show clear evidence for heterogeneity in primitive meteorites (Clayton 1993). This heterogeneity is perhaps best explained by self-shielding of molecular CO gas from UV photodissociation at the surface of the solar nebula (Clayton 2002; Lyons & Young 2005; however, see Ali & Nuth 2007 for an opposing view) or in the presolar molecular cloud (Yurimoto & Kuramoto 2004). Oxygen isotopic anomalies formed at the outer surfaces of the solar nebula by definition imply a spatially heterogeneous initial distribution, perhaps capable of explaining the entire range of stable oxygen isotope ratios through mixing between  $^{16}\text{O}$ -rich and  $^{16}\text{O}$ -poor reservoirs (e.g.,

Sakamoto et al., 2007).

We present here a new set of three dimensional hydrodynamical models of mixing and transport in a protoplanetary disk that demonstrate how the required large-scale transport and mixing may have occurred in the solar nebula. These models are similar to those of Boss (2004, 2007) except that in the new models, the disk is assumed to extend from 1 AU to 10 AU, instead of from 4 AU to 20 AU, in order to better represent the regions of the nebula of most interest for high temperature thermal processing and meteorite formation.

## 2 Numerical Methods

The calculations were performed with a numerical code that uses finite differences to solve the three dimensional equations of hydrodynamics, radiative transfer, and the Poisson equation for the gravitational potential. Detailed equations of state for the gas (primarily molecular hydrogen) and dust grain opacities are employed in the models. Radiative transfer is handled in the diffusion approximation, which is valid near the disk midplane and throughout most of the disk, because of the high vertical optical depths. Artificial viscosity is not employed. A color equation is solved in order to follow the evolution of initially spatially heterogeneous tracers, such as SLRI. The color equation is identical to the density equation, except that the color field is a passive field (a dye) and does not act back on the evolution of the disk. The energy equation is solved explicitly in conservation law form, as are the other hydrodynamic equations. The code is the same as that used in previous studies of mixing and transport in disks (Boss 2004, 2007), and has been shown to be second-order-accurate in both space and time through convergence testing (Boss & Myhill 1992).

The equations are solved on a three dimensional, spherical coordinate grid. The number of grid points in each spatial direction is:  $N_r = 51$ ,  $N_\theta = 23$  in  $\theta = 0^\circ$  to  $90^\circ$ , and  $N_\phi = 256$ . The radial grid is uniformly spaced between 1 and 10 AU, with boundary conditions at both the inner and outer edges chosen to absorb radial velocity perturbations. The  $\theta$  grid is compressed into the midplane to ensure adequate vertical resolution ( $\theta = 0.3^\circ$  at the midplane). The  $\phi$  grid is uniformly spaced, to prevent any bias in the azimuthal direction. The central protostar wobbles in response to the growth of nonaxisymmetry in the disk, thereby rigorously preserving the location of the center of mass of the star and disk system. The number of terms in the spherical harmonic expansion for the gravitational potential of the disk is  $N_{\text{ym}} = 32$ .

In some of the models, diffusion of the dust grains carrying the SLRI or oxygen isotope anomalies with respect to the disk gas is modeled through a modi-

cation of the color equation (Boss 2004, 2007). This modification consists of adding a diffusion term (second space derivative of the color field), multiplied by an appropriate diffusion coefficient  $D$ , which is approximated by the eddy viscosity of a classical viscous accretion disk:  $D = \nu_{\text{turb}} h$ , where  $\nu_{\text{turb}}$  = disk turbulent viscosity parameter,  $h$  = disk scale height, and  $c_s$  = isothermal sound speed at the disk midplane. For typical nebula values at 5 to 10 AU ( $h \approx 1$  AU,  $T \approx 100$  K,  $c_s \approx 6 \times 10^4$  cm s<sup>-1</sup>), the eddy diffusivity becomes  $D \approx 10^{18}$  cm<sup>2</sup> s<sup>-1</sup>.

### 3 Initial Conditions

The models consist of a  $1 M_{\odot}$  central protostar surrounded by a protoplanetary disk with a mass of  $0.047 M_{\odot}$  between 1 and 10 AU. The underlying disk structure is the same as that of the disk extending from 4 AU to 20 AU in the models of Boss (2004, 2007). Disks with similar masses and surface densities appear to be necessary to form gas giant planets by either core accretion (e.g., Inaba et al. 2003) or by disk instability (e.g., Boss et al. 2002). Chemical species observed in comets set an upper limit for disk midplane temperatures in the outer disk of  $\approx 50$  K (Boss 1998). The combination of a disk massive enough to form gas giant planets and the maximum temperatures consistent with cometary speciation implies that the solar nebula was at least marginally gravitationally unstable. Astronomical observations have long indicated that protoplanetary disks have masses in the range of 0.01 to  $0.1 M_{\odot}$ , (e.g., Kitamura et al. 2002), but only more recently has it become apparent that these disk masses appear to be underestimated by factors of up to 10 (Andrews & Williams 2007), which is reassuring, given the high frequency of extrasolar gas giant planets and the need for sufficiently massive disks to explain their formation.

The disks start with an outer disk temperature  $T_o = 40$  K, leading to a minimum in the Toomre  $Q$  ( $Q = c_s^3 / (G \Sigma \Omega)$ , where  $\Omega$  is the disk angular velocity,  $c_s / T^{1/2}$  is the sound speed,  $G$  is the gravitational constant, and  $\Sigma$  is the disk gas surface density) value of 1.43 at 10 AU; inside 6.5 AU,  $Q$  rises to higher values because of the much higher disk temperatures closer to the protosun. A  $Q$  value of 1.43 implies marginal instability to the growth of gravitationally-driven perturbations, while high values of  $Q$  imply a high degree of gravitational stability. These disk models therefore represent marginally gravitationally unstable disks, where strong spiral arms are expected to form on a dynamical (rotational) time scale, and dominate the subsequent evolution of the disk.

A color field representing SLRI or oxygen anomalies is sprayed onto the outer surface of the disk (or injected into the midplane in one model) at a radial

distance of either 2.2 or 8.6 AU, into a 90 degree (in the azimuthal direction) sector of a ring of width 1 AU, simulating the arrival of a Rayleigh-Taylor finger of supernova ejecta (e.g., Vanhala & Boss 2002), a spray of hot grains lofted by the X-wind bipolar outflow (Shu et al. 2001), or a region of the disk's surface that has undergone oxygen isotope fractionation. One of the models includes the effects of the diffusion of the color field with respect to the gaseous disk by a generic turbulent viscosity characterized by  $\alpha = 0.0001$ . This low value is small enough to have only a very minor effect on the color field (Boss 2004, 2007). SLRI, refractory grains, or oxygen anomalies that reside in the gas or in particles with sizes of mm to cm or smaller will remain effectively tied to the gas over timescales of  $\sim 1000$  yrs or so, because the relative motions caused by gas drag result in differential migration by distances of less than 0.1 AU in 1000 yrs, which is negligible compared to the distances they are transported by the gas in that time, justifying their representation by the color field.

## 4 Results

We present here the results of four models. Two models represent initial heterogeneity of the color field on the disk surface at distances of either 2 AU (model 2S) or 9 AU (model 9S) with  $\alpha = 0$ , as well as a third model with 9 AU surface injection with nonzero diffusivity  $\alpha = 0.0001$  (model 9SD). The fourth model assumes the initial heterogeneity exists in the disk's midplane at 2 AU (model 2M), as would be appropriate for refractory grains heated by the hot inner disk. We shall see that whether or not  $\alpha = 0$  or 0.0001 makes little difference to the outcome, as the evolution is dominated by the actions of the gravitational torques from the spiral arms that form. Similarly, whether the color field starts at the disk's surface or midplane makes little difference, as the vertical convective-like motions in these disks rapidly mix the color field upward and downward on a time scale comparable to the orbital period (Boss 2004, 2007).

The color fields shown in the figures represent the number density of small solids (e.g., chondrules, CAIs, ice grains, or their precursor grain aggregates) in the disk carrying SLRI, refractory minerals, or oxygen isotope anomalies, which evolve along with the disk's gas.

Fig. 1 shows how the initial color fields are limited to 90 degree arcs in either the midplane or on the surface of the disks. Fig. 2 shows the midplane color field for model 2S after 385 yrs. Even though the color was initially sprayed onto the surface of model 2S at an orbital distance of 2 AU, the color is rapidly transported down to the disk's midplane by convective-like motions (Boss 2007). In addition, the net effect of the evolution of this marginally

gravitationally unstable disk is to transport the color field inward and outward to the disk boundaries at 1 AU and 10 AU in less than 385 yr. The color field in the innermost disk is depleted by its accretion onto the central protostar, while the color that is transported outward is forced to pile up at the outer disk boundary. This model demonstrates clearly the rapid outward (and upstream with respect to the inward accretion flow of disk gas) transport of small grains from the hot inner disk to the cooler outer disk regions, on time scales of less than 1000 yr.

The color field shown in Fig. 2 represents, e.g., the number density of SLR I in a disk after 385 yr of evolution following an injection event. Given the strong gradients in the color fields evident in Fig. 2, it is clear that the color field is highly spatially heterogeneous. This is because the underlying gas density distribution is equally highly non-axisymmetric and the gas density is the mechanism that drives the transport of the color field. However, cosmological SLR I abundances typically are given as ratios, i.e.,  $^{26}\text{Al}/^{27}\text{Al}$ , where the SLR I  $^{26}\text{Al}$  is derived from the injection event, while the reference stable isotope  $^{27}\text{Al}$  is presumably derived primarily from a well-mixed presolar cloud and so is homogeneous with respect to the original gas disk. [Additional  $^{27}\text{Al}$  would be expected to accompany any  $^{26}\text{Al}$  derived from a supernova source, though not from an X-wind source.] In order to determine the variations in the SLR I ratio  $^{26}\text{Al}/^{27}\text{Al}$ , then, the color field must be normalized by the gas density. This has been done for model 2S in Fig. 3, which shows the log of the color/gas ratio at a time of 8.4 yr, shortly after the injection event. The high degree of initial spatial heterogeneity of the ratio  $^{26}\text{Al}/^{27}\text{Al}$  is obvious. However, Fig. 4 shows that after 385 yr of evolution (the same time as in Fig. 2), the color/gas ratio has become remarkably uniform throughout the midplane of the disk, with variations of less than 0.1 in the log, or no more than a factor of 1.26. Even variations this large only occur close to the inner and outer boundary where there is very little color and even less gas density, so that the ratio becomes large. Such regions contain essentially no gas and so are negligible. This model shows that the color field can become homogeneous with respect to the disk gas in a few hundred years of evolution in a marginally gravitationally unstable disk.

An important quantity to calculate in this regard is the dispersion of the color/gas density ratio from its mean value (Boss 2007), in order to make a more quantitative comparison with isotopic measurements. Fig. 5 shows the time evolution of the level of spatial heterogeneity in, e.g., SLR I ratios such as  $^{26}\text{Al}/^{27}\text{Al}$  following a single SLR I injection event, for models 2S and 2M. Fig. 5 plots the square root of the sum of the squares of the color field divided by the gas density subtracted from the mean value of the color field divided by the gas density, where the sum is taken over the midplane grid points and is normalized by the number of grid points being summed over. The sum excludes the regions closest to the inner and outer boundaries, as well as regions with

disk gas densities less than  $10^{-12} \text{ g cm}^{-3}$ , as the low gas densities in these regions skew the calculations of the dispersion of the ratio of color to disk gas, and these regions contain comparatively little gas and dust.

Fig. 5 shows that the dispersions for both models 2S and 2M follow similar time evolutions, starting from high initial values. While model 2M has not yet been continued as far as model 2S, model 2S shows that the expectation is that in both models, the dispersion will fall to a level of 5% to 10%, as was found in the larger-scale (4 AU to 20 AU) disk models of Boss (2007).

We now turn to the models where the color field was initiated at orbital distances centered on 9 AU. Fig. 6 shows the result for model 9SD just 16 yr after injection, when the color has already been transported down to the midplane, as well as inward to orbital distances of only a few AU. The spiral-like nature of the color field is a clear indicator of the transport mechanism responsible for this rapid movement. Fig. 7 shows how the color/gas density ratio for model 9SD has become considerably more homogenized after 210 yr of evolution, while Fig. 8 shows that nearly complete homogenization of the color field is achieved after 1526 yrs of evolution, with some residual heterogeneity remaining in the inner disk. Fig. 9 shows the color/gas density ratio for model 9S, which was identical to model 9SD, except for having  $\beta = 0$ , compared to  $\beta = 0.0001$  for model 9SD. Evidently this small level of diffusivity of the color field with respect to the gas density has little appreciable effect on the evolution of the color field, as was also found by Boss (2007).

Finally, Fig. 10 displays the time evolution of the dispersions for models 9S and 9SD. Both models demonstrate that the dispersion does not approach zero, as might be expected, but rather falls to a level on the order of 10%, where the dispersion appears to reach a steady state. This implies that gravitational mixing is not 100% efficient and is unable to completely homogenize an initial spatial heterogeneity. Gravity is a long-range force, only able to drive mixing over length scales where large density variations occur, i.e., over length scales comparable to the disk's spiral arms. These spiral arms tend to have radial length scales of no less than an AU or so, much larger than the radial extent of a grid cell (0.18 AU), which appears to lead to the large-scale granularity at the 10% level seen in Fig. 10.

## 5 Conclusions

The discovery of refractory minerals in Comet Wild 2 by the Stardust Mission (Brownlee et al. 2006) is consistent with the rapid (less than 1000 yr), large-scale (10s of AU) outward transport of small dust grains in a marginally gravitationally unstable disk. Such large-scale transport also seems to be re-



quired to explain observations of thermally processed, crystalline silicates in comets and protoplanetary disks (e.g., Nuth & Johnson 2006; van Boekel et al. 2005; Merín et al. 2007). Marginally gravitationally unstable disks have the additional feature of providing a robust source of shock fronts capable of thermally processing solids into chondrules (Desch & Connolly 2002; Boss & Durisen 2005). Furthermore, the degree of spatial heterogeneity in the solar nebula required for the use of the  $^{26}\text{Al}/^{27}\text{Al}$  chronometer and for the survival of the oxygen isotope anomalies is consistent with the results of these models of mixing and transport of initially highly spatially heterogeneous tracers in a marginally gravitationally unstable disk (Boss 2007). Such a disk appears to be required for the formation of Jupiter by either the core accretion (Inaba et al. 2003) or disk instability (Boss et al. 2002) mechanisms. Marginally gravitationally unstable disk models provide a physical mechanism for self-consistent calculations of the mixing and transport of dust grains across the planet-forming region of the solar nebula.

Mass accretion rates of the disk onto the central protostar are highly variable in marginally gravitationally unstable models, ranging from rates of  $10^{-6} M_{\odot}/\text{yr}$  to  $10^{-5} M_{\odot}/\text{yr}$ , much higher than the typical stellar mass accretion rate of  $10^{-8} M_{\odot}/\text{yr}$  for a classical T Tauri star, but comparable to the rates inferred for T Tauri stars during their periodic FU Orionis outbursts (Boss 1996). Recent observations suggest that most T Tauri disks have lifetimes of no more than 1 Myr (Cieza et al. 2007). Combined with a disk mass of  $0.1 M_{\odot}$ , this suggests a time-averaged mass accretion rate for solar-mass T Tauri stars of  $10^{-7} M_{\odot}/\text{yr}$ . A disk would then need to experience phases of gravitational instability lasting roughly 1% to 10% of its lifetime in order to accomplish the mass transport implied by these estimates. Phases of gravitational instability are thus expected to be transient phases, but robust and frequent enough to achieve the disk mixing and transport processing described in this paper.

I thank Sasha Krot and a second referee for their improvements to the paper, and Sandy Keiser for her computer wizardry. This research was supported in part by the NASA Planetary Geology and Geophysics Program under grant NNG 05GH 30G and by the NASA Origins of Solar Systems Program under grant NNG 05G 110G, and is contributed in part to the NASA Astrobiology Institute under grant NCC 2-1056. Calculations were performed on the Carnegie Alpha Cluster, which was supported in part by NSF MRI grant AST-9976645.

## References

- [1] Ali, A., & Nuth, J. A., The oxygen isotope effect in the earliest processed solids in the solar system : is it a chemical mass-independent process?, 2007, *Astronomy*

- & Astrophysics, 467, 919-923.
- [2] Amelin, Y., Krot, A.N., Hutcheon, I.D., & Ulyanov, A.A., Lead Isotopic Ages of Chondrules and Calcium-Aluminum-Rich Inclusions, 2002, *Science*, 297, 1678-1683.
- [3] Andreasen, R., & Sharma, M., Mixing and Homogenization in the Early Solar System: Clues from Sr, Ba, Nd, and Sm Isotopes in Meteorites, 2007, *Astrophysical Journal*, 665, 874-883.
- [4] Andrews, S.M., & Williams, J.P., High-Resolution Submillimeter Constraints on Circumstellar Disk Structure, *Astrophysical Journal*, 659, 705-728.
- [5] Bizzarro, M., Baker, J.A., & Haack, H., Mg isotope evidence for contemporaneous formation of chondrules and refractory inclusions, 2004, *Nature*, 431, 275-278.
- [6] Boss, A.P., Evolution of the Solar Nebula. III. Protoplanetary Disks Undergoing Mass Accretion, 1996, *Astrophysical Journal*, 469, 906-920.
- [7] Boss, A.P., Temperatures in Protoplanetary Disks, 1998, *Annual Reviews of Earth and Planetary Science*, 26, 53-80.
- [8] Boss, A.P., Evolution of the Solar Nebula. VI. Mixing and Transport of Isotopic Heterogeneity, 2004, *Astrophysical Journal*, 616, 1265-1277.
- [9] Boss, A.P., Evolution of the Solar Nebula. VIII. Spatial and Temporal Heterogeneity of Short-lived Radioisotopes and Stable Oxygen Isotopes, 2007, *Astrophysical Journal*, 660, 1707-1714.
- [10] Boss, A.P., & Durisen, R.H., Chondrule-Forming Shock Fronts in the Solar Nebula, A Possible Unified Scenario for Planet and Chondrite Formation, 2005, *Astrophysical Journal*, 621, L137-L140.
- [11] Boss, A.P., & Myhill, E.A., Protostellar Hydrodynamics, Constructing and Testing a Spatially and Temporally Second Order Accurate Method. I. Spherical Coordinates, 1992, *Astrophysical Journal Supplement Series*, 83, 311-327.
- [12] Boss, A.P., Wetherill, G.W., & Haghighipour, N., Rapid Formation of Ice Giant Planets, 2002, *Icarus*, 156, 291-295.
- [13] Brownlee, D.E. et al., Comet 81P/Wild 2 Under a Microscope, 2006, *Science*, 314, 1711-1716.
- [14] Ciesla, F.J., Outward Transport of High-Temperature Materials Around the Midplane of the Solar Nebula, 2007, *Science*, 318, 613-615.
- [15] Ciesla, F.J., & Cuzzi, J.N., The evolution of the water vapor distribution in a viscous protoplanetary disk, 2006, *Icarus*, 181, 178-204.
- [16] Cieza, L., et al., The SPITZER c2d Survey of Weak-Line T Tauri Stars. II. *Astrophysical Journal*, 667, 308-328.

- [17] Clayton, R. N., Oxygen Isotopes in Meteorites, 1993, *Annual Reviews of Earth Planetary Science*, 21, 115-149.
- [18] Clayton, R. N., Self-shielding in the solar nebula, 2002, *Nature*, 415, 860-861.
- [19] Desch, S. J., & Connolly, H. C., Jr., A model of the thermal processing of particles in solar nebula shocks: Application to the cooling rates of chondrules, 2002, *Meteoritics & Planetary Science*, 37, 183-207.
- [20] Gail, H.-P., Radial mixing in protoplanetary disks III. Carbon dust oxidation and abundance of hydrocarbons in comets, 2002, *Astronomy & Astrophysics*, 390, 253-265.
- [21] Halliday, A., The clock's second hand, 2004, *Nature*, 431, 253-254.
- [22] Huss, G. R., & Wasserburg, G. J., Aluminosilicate systematics of CAIs, POI, and ferromagnesian chondrules from Ningqiang, 2003, *Meteoritics & Planetary Science*, 38, 35-48.
- [23] Inaba, S., Wetherill, G. W., & Ikoma, M., Formation of gas giant planets, core accretion models with fragmentation and planetary envelope, 2003, *Icarus*, 166, 46-62.
- [24] Kitamura, Y., et al., Investigation of the Physical Properties of Protoplanetary Disks Around T Tauri Stars by a 1.4 m Second Imaging Survey, 2002, *Astrophysical Journal*, 581, 357-380.
- [25] Krot, A. N., Yurimoto, H., Hutcheon, I. D., & MacPherson, G. J., Chronology of the early Solar System from chondrule-bearing calcium-aluminum-rich inclusions, 2005, *Nature*, 434, 998-1001.
- [26] Krot, A. N., et al., Evolution of Oxygen Isotopic Composition in the Inner Solar Nebula, 2005, *Astrophysical Journal*, 622, 1333-1342.
- [27] Lyons, J. R., & Young, E. D., CO self-shielding as the origin of oxygen isotope anomalies in the early solar nebula, 2005, *Nature*, 435, 317-320.
- [28] Matsumura, S., & Pudritz, R. E., Dead zones and extrasolar planetary properties, 2006, *Monthly Notices Royal Astronomical Society*, 365, 572-584.
- [29] Meren, B., et al., Abundant Crystalline Silicates in the Disk of a Very Low Mass Star, 2007, *Astrophysical Journal*, 661, 361-367.
- [30] Mostefaoui, S., Lugmair, G., & Hoppe, P.,  $^{60}\text{Fe}$ , A Heat Source for Planetary Differentiation From a Nearby Supernova Explosion, 2005, *Astrophysical Journal*, 625, 271-277.
- [31] Nuth, J. A., & Johnson, N. M., Crystalline silicates in comets, How did they form?, 2006, *Icarus*, 180, 243-250.
- [32] Sakamoto, N., Seto, Y., Itoh, S., Kuramoto, K., Fujino, K., Nagashima, K., Krot, A. N., & Yurimoto, H., Remnants of the Early Solar System Water Enriched in Heavy Oxygen Isotopes, 2007, *Science*, 317, 231-233.

- [33] Simon, S. B., Davis, A. M., Grossman, L., & Zinner, E. K., Origin of hibonite-pyroxene spherules found in carbonaceous chondrites, 1998, *Meteoritics & Planetary Science*, 33, 411-424.
- [34] Shu, F. H., Shang, H., Gounelle, M., Glassgold, A. E., & Lee, T., The Origin of Chondrules and Refractory Inclusions in Chondritic Meteorites, 2001, *Astrophysical Journal*, 548, 1029-1050.
- [35] Tachibana, S., & Huss, G. R., The Initial Abundance of  $^{60}\text{Fe}$  in the Solar System, 2003, *Astrophysical Journal*, 588, L41-L44.
- [36] Thrane, K., Bizzarro, M., & Baker, J. A., Extremely Brief Formation Interval for Refractory Inclusions and Uniform Distribution of  $^{26}\text{Al}$  in the Early Solar System, 2006, *Astrophysical Journal*, 646, L159-L162.
- [37] Tschamuter, W. M., & Gail, H.-P., 2-D preplanetary accretion disks I. Hydrodynamics, chemistry, and mixing processes, 2007, *Astronomy & Astrophysics*, 463, 369-392.
- [38] van Boekel, R., et al., A 10  $\mu\text{m}$  spectroscopic survey of Herbig Ae star disks: Grain growth and crystallization, 2005, *Astronomy & Astrophysics*, 437, 189-208.
- [39] Vanhala, H. A. T., & Boss, A. P., Injection of Radioactivities into the Forming Solar System, 2002, *Astrophysical Journal*, 575, 1144-1150.
- [40] Weidenschilling, S. J., Formation processes and time scales for meteorite parent bodies, 1988, in *Meteorites and the Early Solar System*, eds. J. F. Kerridge & M. S. Matthews (Tucson, Univ. of Arizona Press), pp. 348-371.
- [41] Yin, Q.-Z., Predicting the Sun's Oxygen Isotope Composition, 2004, *Science*, 305, 1729-1730.
- [42] Yokoyama, T., Rai, V. K., Alexander, C. M. O'D., Lewis, R. S., Carlson, R. W., Shirey, S. B., Thiemens, M. H., & Walker, R. J., 2007, Oxygen isotope evidence for uniform distribution of s- and r-process components in the early solar system, *Earth & Planetary Science Letters*, 259, 567-580.
- [43] Young, E. D., et al., Supra-canonical  $^{26}\text{Al}/^{27}\text{Al}$  and the Residence Time of CA Is in the Solar Protoplanetary Disk, 2005, *Science*, 308, 223-227.
- [44] Yurimoto, H., & Kuramoto, K., Molecular Cloud Origin for the Oxygen Isotope Heterogeneity in the Solar System, 2004, *Science*, 305, 1763-1766.

CMAX= 1.0000    CONDIF= 0.1000    R= 0.15E+15

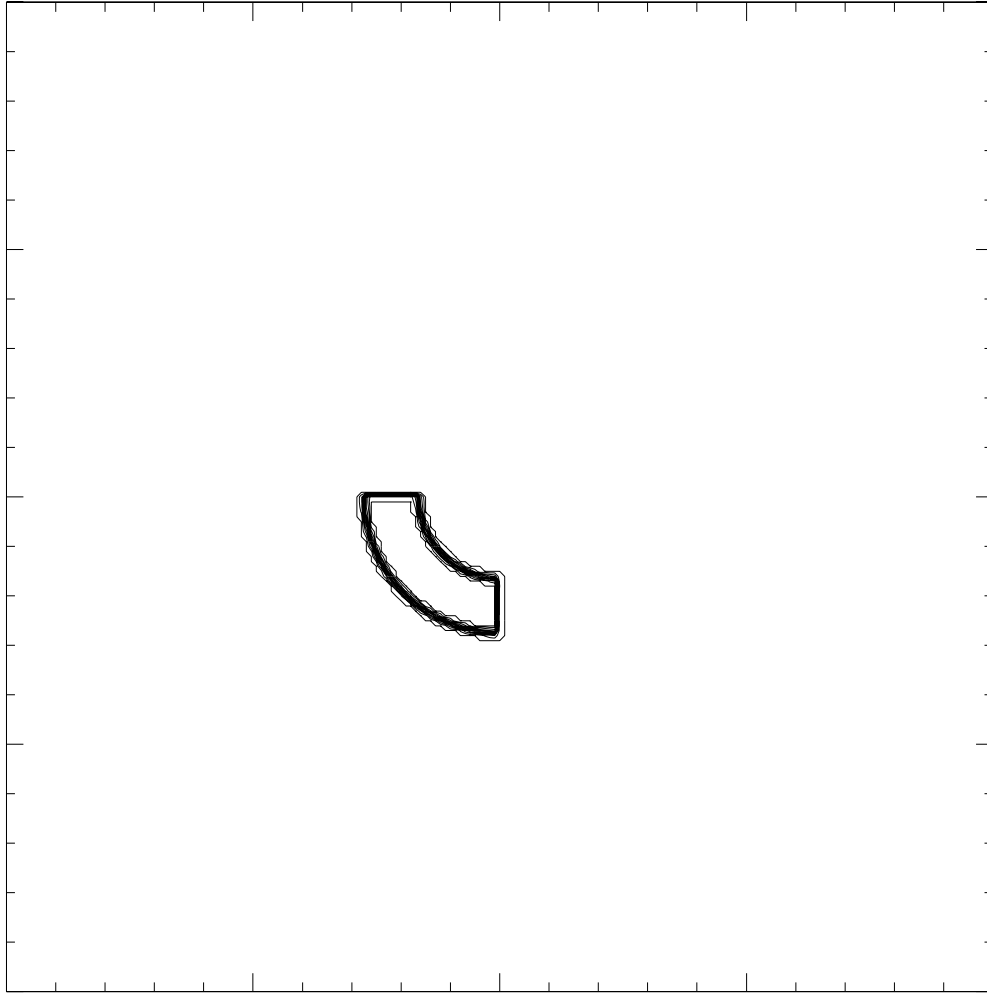


Figure 1. Model 2M at 0 yr, showing linear contours of the color field density (e.g., number of atoms of  $^{26}\text{Al cm}^{-3}$ ) in the disk midplane at the instant when the color field was injected into the disk's midplane in a 90 degree azimuthal sector between 1.6 and 2.8 AU. Region shown is 10 AU in radius (R) with a 1 AU radius inner boundary. In this Figure, the contours represent changes in the color field density by 0.1 units (CONDIF) on a scale normalized by the initial color field density of 1.0, up to a maximum value of 1.0 (CMAX).

CMAX= 0.1000    CONDIF= 0.0010    R= 0.15E+15

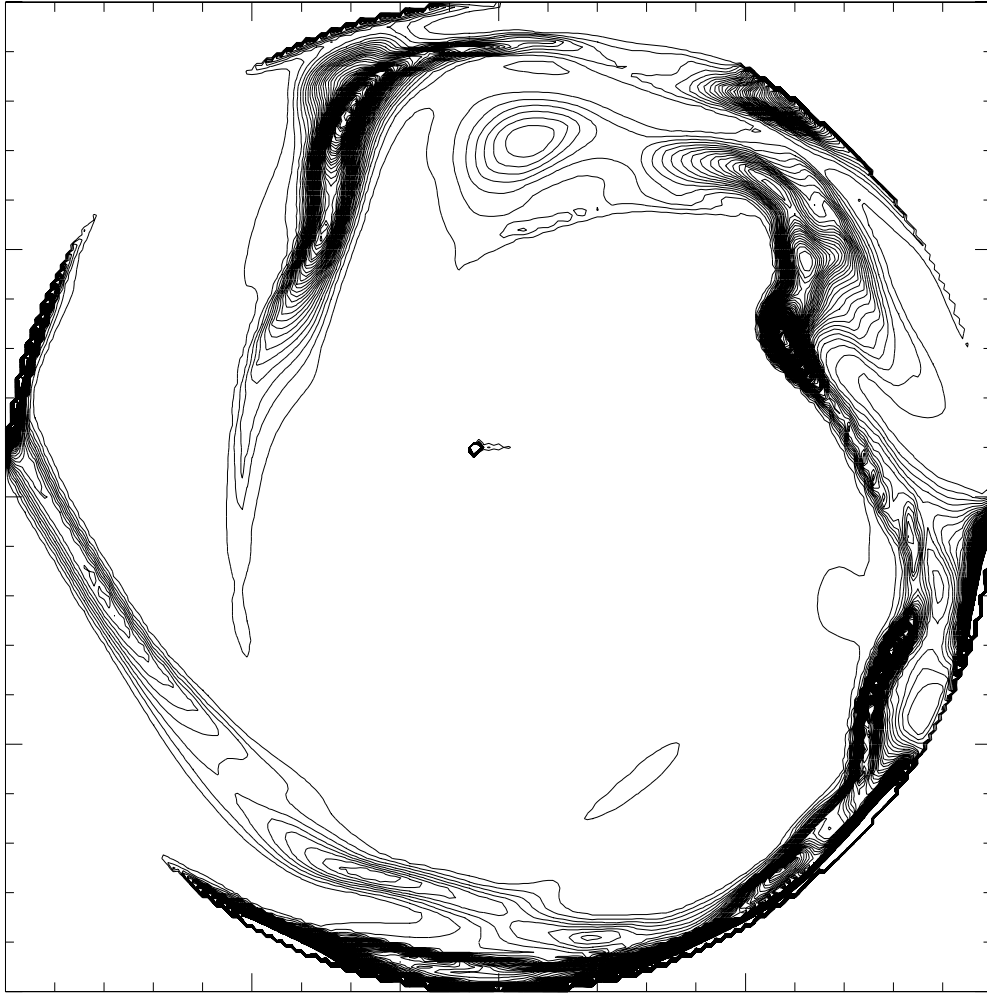


Figure 2. Same as Fig. 1, but for model 2S after 385 yr. The color field has spread outward to the edge of the disk. The spatial distribution is highly heterogeneous, with the highest concentrations residing inside the spiral arms of the disk and on the edge of the disk, where it is artificially not allowed to move farther outward.

CONMAX= 10.0 CONDIF=0.1000 R= 0.15E+15

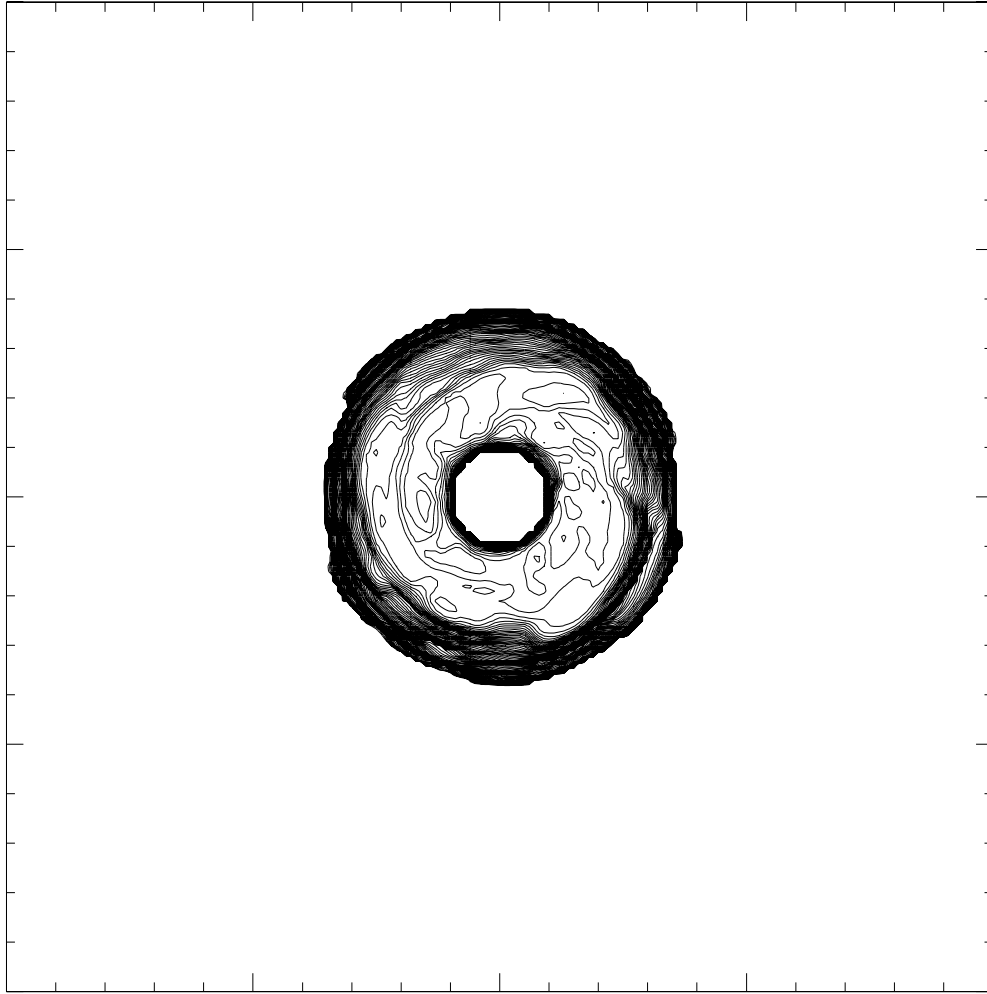


Figure 3. Logarithmic contours of the color field density divided by the disk gas density (i.e.,  $\log$  of the abundance ratio  $^{26}\text{Al}/^{27}\text{Al}$ ) for model 2S at a time of 8.4 yr, plotted in the same manner as in Fig. 1. Contours represent changes by factors of 1.26 up to a maximum value of 10.0, on a scale defined by the gas disk density. At this early time, the color/gas ratio is highly spatially heterogeneous, as the color field is still confined to the innermost disk, where it was first injected.

CONMAX= 10.0 CONDIF=0.1000 R= 0.15E+15

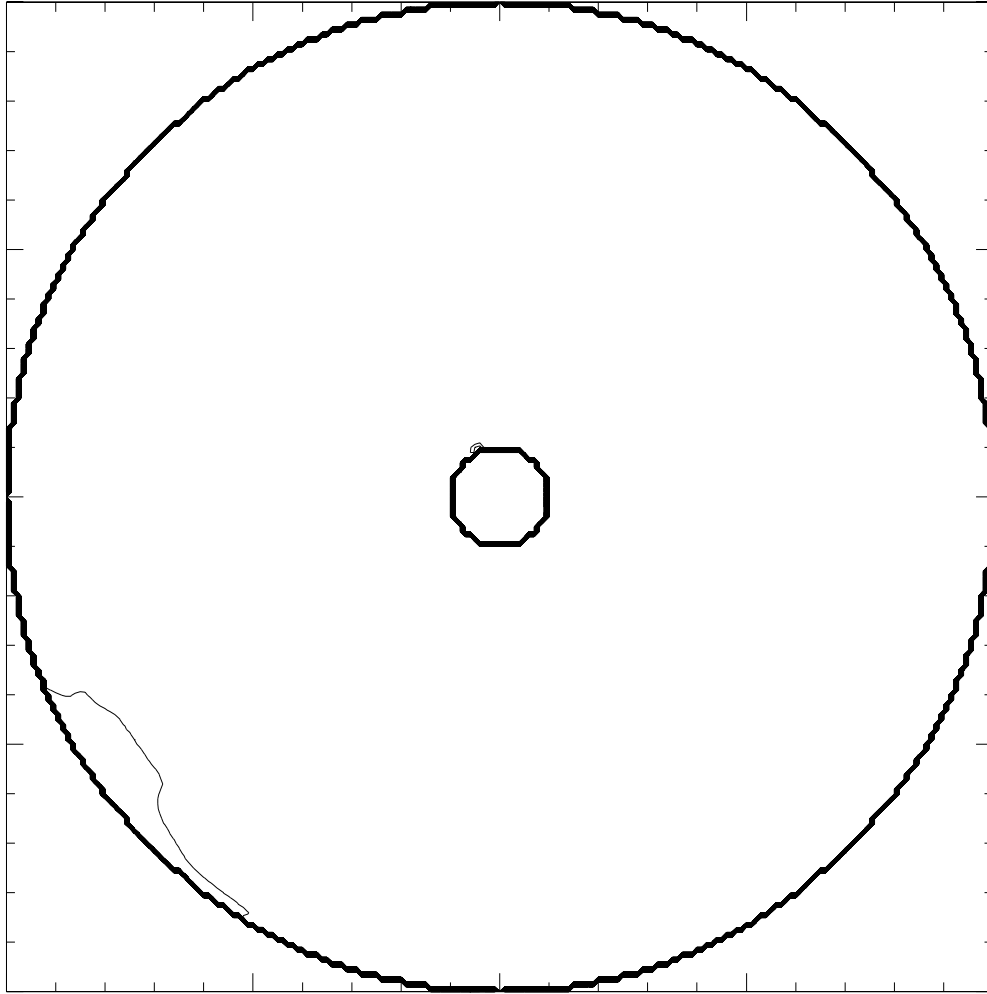


Figure 4. Same as Fig. 3 for model 2S, but after 385 yr of evolution. The color/gas ratio is now nearly homogeneous throughout the entire disk, except for small regions along the inner and outer boundaries, which are clearly artificial boundary effects.



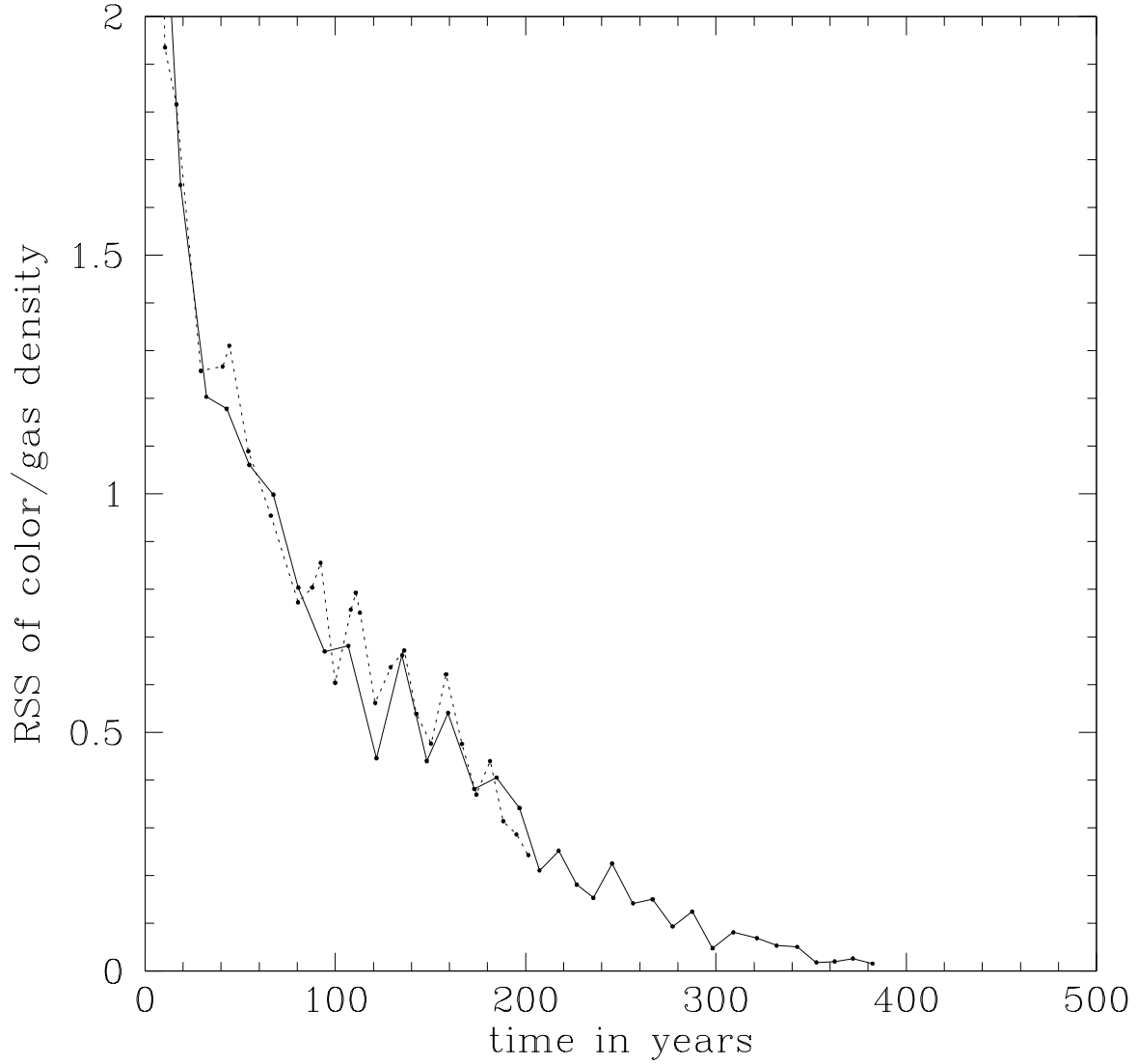


Figure 5. Time evolution of the dispersion from the mean (i.e., standard deviation, or the root of the sum of the squares [RSS] of the differences from the mean) of the color field density divided by the gas density (e.g.,  $^{26}\text{Al}/^{27}\text{Al}$  abundance ratio) in the disk midplane in models 2S (solid) and 2M (dashed). The color field is sprayed onto the disk surface or injected into the disk midplane at a time of 0 yr. Starting from high values (RSS shortly after 0 yrs is  $\gg 1$ ), the dispersion decreases on a timescale of  $\sim 300$  yrs, dropping to a value of  $\sim 5\%$ .

CONMAX= 10.0 CONDIF=0.1000 R= 0.15E+15

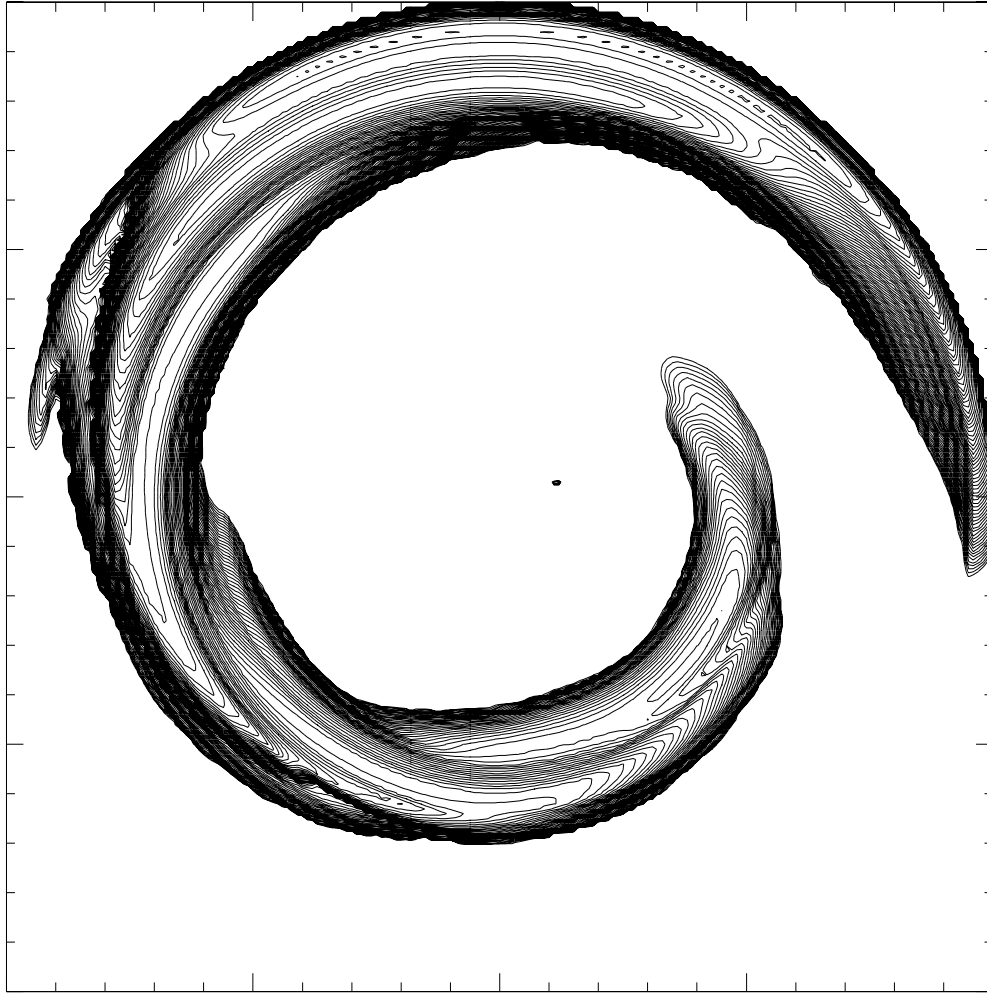


Figure 6. Model 9SD at 16 yr, showing logarithmic contours of the color field density divided by the disk gas density in the disk midplane 16 yr after the color field was sprayed onto the disk's surface in a 90 degree azimuthal sector between 8.1 and 9.1 AU (as in Fig. 1). Region shown is 10 AU in radius ( $R$ ) with a 1 AU radius inner boundary. Contours represent changes by factors of 1.26 up to a maximum value of 10.0, on a scale defined by the gas disk density. At this early time, the color/gas ratio is again highly spatially heterogeneous, as the color field is mostly confined to the outermost disk, where it was first injected, though inward motion toward the central protostar along a single-arm spiral arm is evident.

CONMAX= 10.0 CONDIF=0.1000 R= 0.15E+15

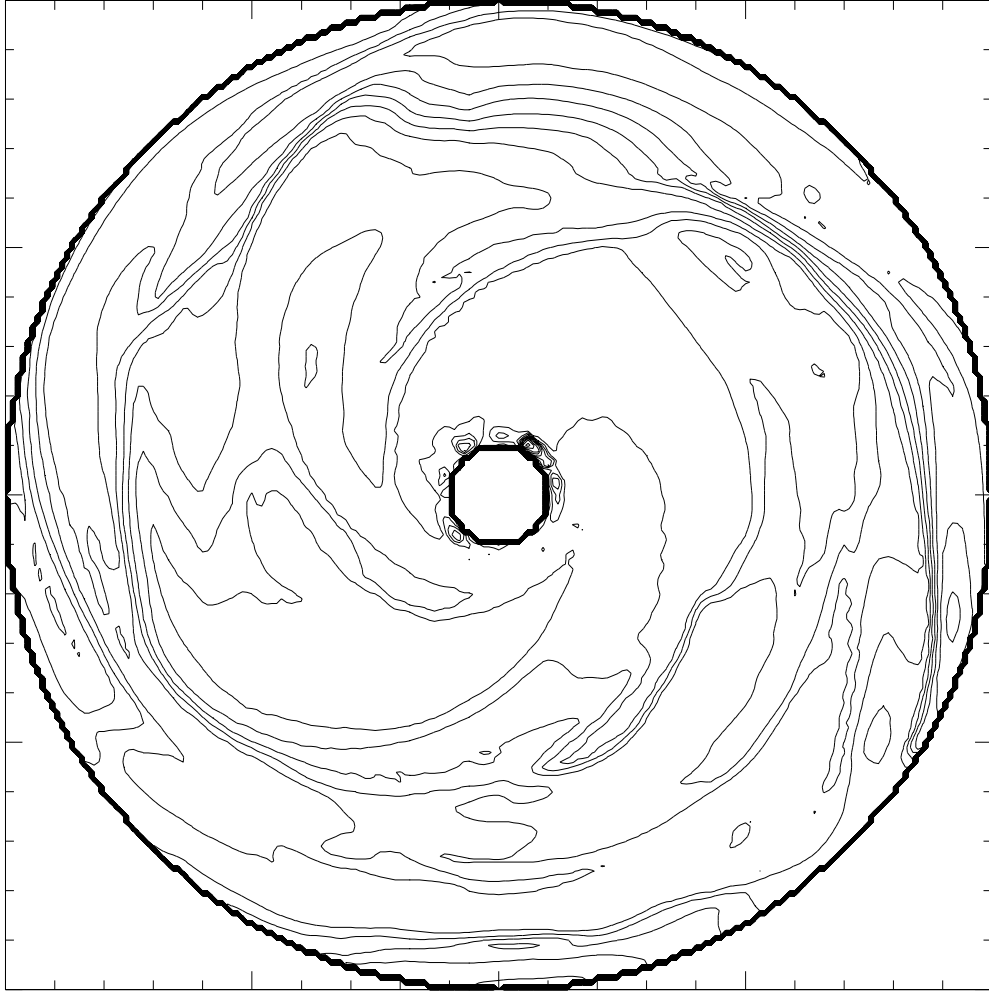


Figure 7. Same as Fig. 6 for model 9SD, but after 210 yr of evolution. The color/gas ratio is approaching spatial homogeneity compared to Fig. 6, as a result of mixing and transport by the disk's spiral arms.

CONMAX= 10.0 CONDIF=0.1000 R= 0.15E+15



Figure 8. Same as Fig. 7 for model 9SD, but after 1526 yr of evolution. The color/gas ratio is now nearly homogeneous throughout the entire disk, except for small regions right along the inner boundary, which is a boundary effect.

CONMAX= 10.0 CONDIF=0.1000 R= 0.15E+15

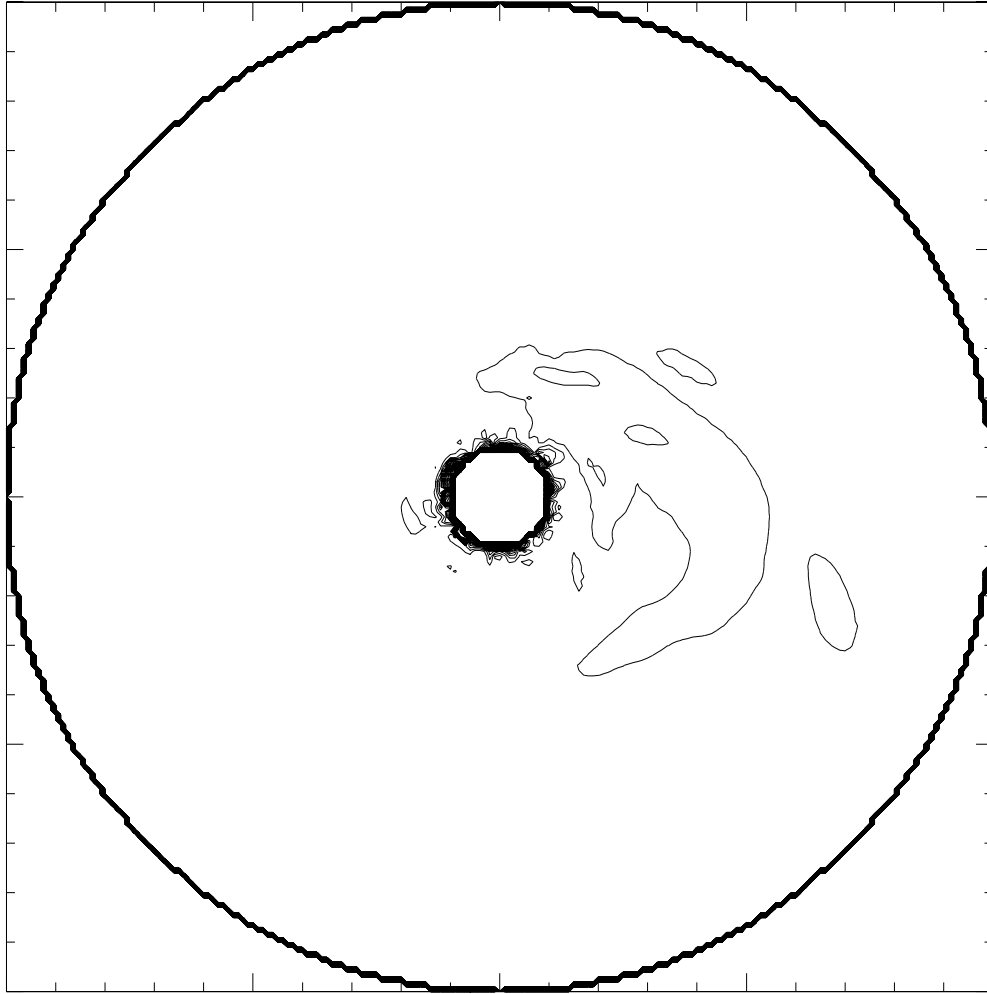


Figure 9. Same as Figure 8, after 1526 yr of evolution, but from model 9S, which had no turbulent diffusion of the color field with respect to the disk gas. Evidently the level of turbulent diffusion in model 9SD has essentially no effect upon the mixing and transport processes.

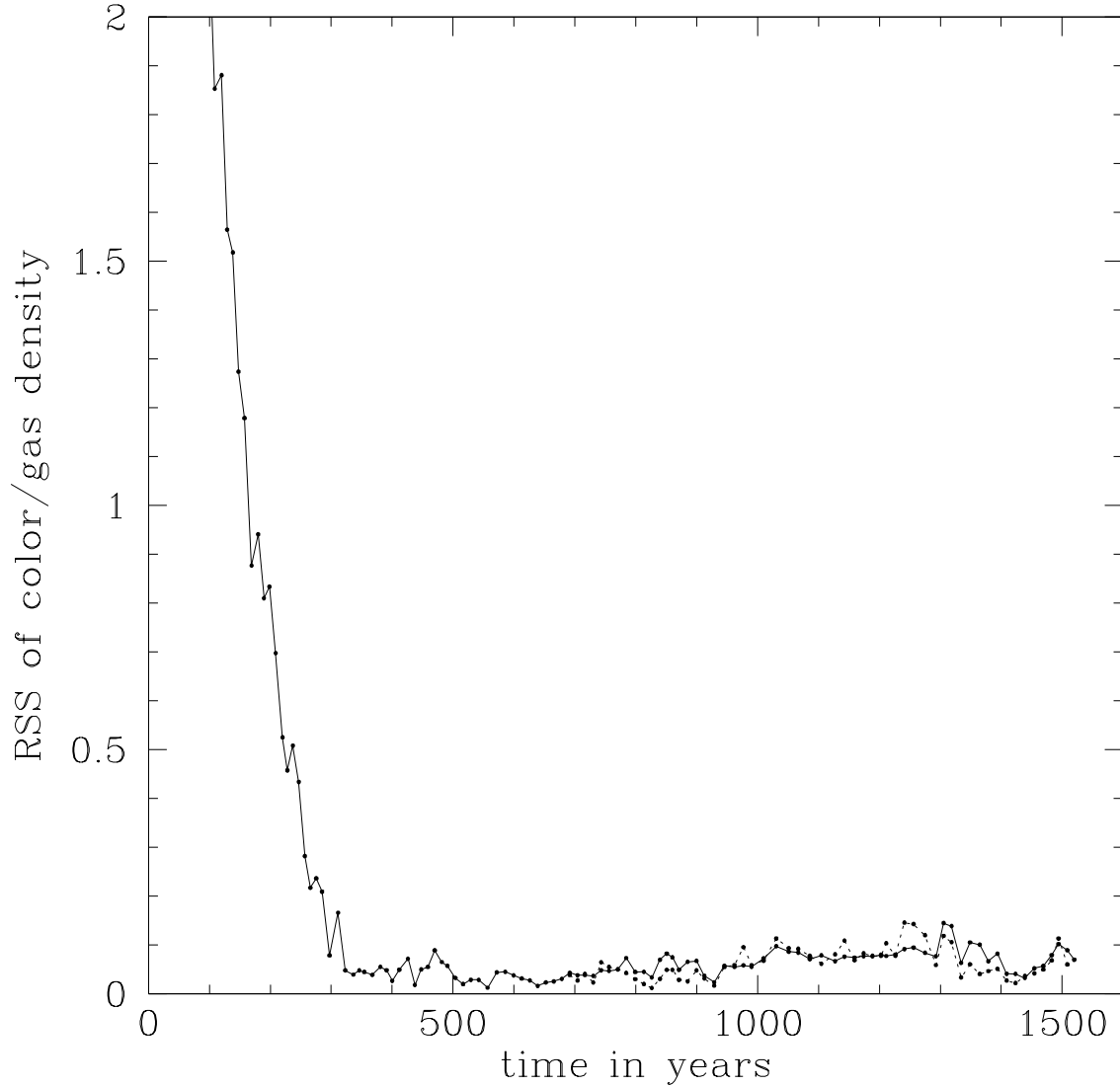


Figure 10. Time evolution of the dispersion from the mean of the color field density divided by the gas density (e.g.,  $^{26}\text{Al}/^{27}\text{Al}$  abundance ratio) in the disk midplane in models 9SD (solid) and 9S (dashed). The color field is sprayed onto the disk surface at a time of 0 yr. The dispersion again decreases on a timescale of  $\sim 300$  yrs, then approaches a steady state value of  $\sim 10\%$ . After 700 yr, the results for model 9S are plotted as well, showing that the non-zero turbulent diffusion in 9SD has no appreciable effect on the steady level reached.